Plant Physiology Preview. Published on July 26, 2012, as DOI:10.1104/pp.112.200311

Running head: Isogenic mapping-by-sequencing

Correspondence:

Dr. Franziska Turck
Max Planck Institute for Plant Breeding Research
Department of Plant Developmental Biology
Carl-von-Linné-Weg 10
50829 Cologne
Germany
turck@mpipz.mpg.de

Dr. Korbinian Schneeberger
Max Planck Institute for Plant Breeding Research
Department of Plant Developmental Biology
Carl-von-Linné-Weg 10
50829 Cologne
Germany
schneeberger@mpipz.mpg.de

Research area: Bioinformatics

Fast isogenic mapping-by-sequencing of EMS-induced mutant bulks

Benjamin Hartwig[1], Geo Velikkakam James[1], Kathryn Konrad[2], Korbinian Schneeberger[1,*], Franziska Turck[1,*]

[1] Max Planck Institute for Plant Breeding Research, Department of Plant Developmental Biology, Max Planck Society, Cologne, Germany

[2] Universität zu Köln, Cologne Center for Genomics (CCG), Cologne, Germany

Footnotes:

1.) We acknowledge financial support from the Max Planck Society and the Deutsche Forschungsgemeinschaft.

2.) Corresponding authors e-mail:

<Franziska Turck> turck@mpipz.mpg.de

<Korbininan Schneeberger> schneeberger@mpipz.mpg.de

Abstract

Mapping-by-sequencing (or SHOREmapping) has revitalized the powerful concept of forward genetic screens in plants. However, as in conventional genetic mapping approaches, mapping-by-sequencing requires phenotyping of mapping populations established from crosses between two diverged accessions. In addition to the segregation of the focal phenotype, this introduces natural phenotypic variation, which can interfere with the recognition of quantitative phenotypes. Here, we demonstrate how mapping-by-sequencing and candidate gene identification can be performed within the same genetic background, using only mutagen-induced changes as segregating markers. Using a previously unknown suppressor of mutants of *like heterochromatin protein 1*(*lhp1*), which in its functional form is involved in chromatin-mediated gene repression, we identified three closely linked ethyl methanesulfonate (EMS)-induced changes as putative candidates. In order to assess allele frequency differences between such closely linked mutations, we introduced deep candidate resequencing (dCARE) using the new Ion Torrent PGM sequencing platform to our mutant identification pipeline and thereby reduced the number of causal candidate mutations to only one. Genetic analysis of two independent additional alleles confirmed that this mutation was causal for the suppression of *lhp1*.

Introduction

In *Arabidopsis thaliana* (Arabidopsis) research, EMS mutagenesis is a powerful tool, which has been widely explored to uncover functionality of many genes in a broad spectrum of pathways (Page and Grossniklaus, 2002). Recent advances in sequencing technology have greatly reduced the time required to pinpoint induced mutations. In a proof of principle experiment, mapping-by-sequencing (SHOREmapping) was first demonstrated on a mutant in the background of the Arabidopsis reference accession Columbia (Col-0) crossed to the diverged accession Landsberg *erecta* (L*er*). A pool of DNA isolated from bulked segregants was sequenced and used for the simultaneous mapping and mutant identification (Schneeberger et al., 2009). This first application was followed by other studies successfully applying similar methods (Cuperus et al., 2010; Austin et al., 2011).

Although all described approaches are straightforward and extremely fast, their application is hindered by the requirement for inter-accession crosses that impedes the success rate of screens based on quantitative traits, such as screens for genetic modifiers. The major obstacle is that the considerable phenotypic variation in F_2 populations from crosses between diverged accessions impairs recognition of mutants with subtle phenotypic alterations. In addition, if genetic screens involve modifiers of a pre-existing mutant, the mapping depends on the availability of the primary mutant in another suitable accession, the introgression of the mutation in such a background or the laborious additional genotyping for the presence of the first-site mutation.

Avoiding these disadvantages, Ashelford and colleagues have demonstrated that the isolation of a causative EMS-induced change is possible by direct resequencing of a complete mutant genome (Ashelford et al., 2011). However, their approach initially resulted in 103 putative causal mutations that had the potential to change the amino acid sequences of 48 putative proteins. In addition, the mutations were clustered in two separate regions of the genome, even though the mutant had been backcrossed four times to the parental line**.**

Recently, Abe *et al.* reduced the large number of candidate mutations by backcrossing of mutant genomes to their non-mutagenized progenitor, followed by sequencing bulk segregants from these crosses (Abe et al., 2012). This drastically reduced the number of causal candidates, however it was not possible to pinpoint the causal change from the sequencing data alone. The main problem remains the short-read coverage at each of the candidate mutations that is typically lower than the number of individuals combined within the bulked DNA. This hinders accurate allele frequency estimations based on the whole-

genome sequencing data alone and thus makes it impossible to distinguish between causal and closely linked mutations.

In this study, we combined isogenic bulk segregant analysis with deep candidate resequencing (dCARE) to facilitate mutation identification of genetic modifiers based on bulked DNA and sequencing data alone. Our approach relies on the assumption that in pools of bulked segregants the causative change occurs with the highest frequency among all EMS induced changes (Fig. 1). Using resequencing data alone, it is not possible to distinguish between the subtle alleles frequencies of EMS changes that are closely linked. However, dCARE of all candidate mutations using the new Ion Torrent sequencing technology enables quick and cost-effective detection of subtle allele frequency differences between closely linked mutations and thus allows identification of causal candidates.

The mutant identified by this fast isogenic mapping approach was isolated as suppressor of developmental aberrations caused by defects in *LIKE HETEROCHROMATIN PROTEIN 1* (*LHP1*), which participates in the Polycomb Group (PcG) gene regulatory pathway in Arabidopsis. Enhancer/suppressor screens have been successfully used to identify genes that play a role in chromatin-mediated gene repression and activation in *Drosophila melanogaster*. For example, many components of the repressive PcG pathway were isolated as genetic enhancers or suppressors of homeotic mutations, whereas components of the trithorax Group (trxG) protein pathway were originally identified as suppressors of PcG related mutations (Landecker et al., 1994; Gildea et al., 2000; Alonso et al., 2007).

Results

Mutant selection for fast isogenic mapping-by-sequencing

We selected an EMS-induced mutant that was isolated as suppressor of the *lhp1* mutant phenotype to validate the isogenic mapping approach. LHP1 is part of one or several distinct POLYCOMB REPRESSIVE COMPLEXES 1 (PRC1s) in Arabidopsis (Xu and Shen, 2008; Bratzel et al., 2010). PRC1s are targeted to nucleosomes that carry lysine 27 tri-methylated H3 (H3K27me3) and the chromo-domain of LHP1 directly binds H3K27me3 (Turck et al., 2007; Zhang et al., 2007; Exner et al., 2009).

Mutated *lhp1* plants display a pleiotropic phenotype. They are shorter, have smaller, downwardly curled leaves, flower earlier than wild-type (WT) independent of day length and form terminal flowers (Kotake et al., 2003). However, the phenotype is relatively mild if compared with that of mutants that have globally reduced H3K27me3 levels or are severely

impaired in their PRC1 function. In these mutant plants, developmental structures are not maintained resulting in a callus-like growth phenotype (Makarevich et al., 2006; Bratzel et al., 2010).

We performed an EMS mutagenesis of the *lhp1-3* (alternative name *tfl2-2*, (Larsson et al., 1998)) mutant to perform a large forward genetic screen for genetic suppressors and enhancers of *lhp1*. Among other mutants, the screen led to the isolation of the EMS-induced *alp1* (*antagonist of lhp1 1*);*lhp1* double mutant as a suppressor of the *lhp1* phenotype. Height, cauline and rosette leaf size and silique length were increased in *alp1*;*lhp1* compared to the *lhp1* single mutant resulting in an intermediate phenotype between the WT Col-0 reference and the *lhp1* mutant (Fig.2 A-C).

Double-mutant plants flowered earlier than Col-0 WT plants but later than *lhp1* mutants in our screening conditions (Fig. 2D). Early flowering of *lhp1* mutant plants is caused by the up-regulation of *FLOWERING LOCUS T* (*FT*) expression (Kotake et al., 2003). Obvious candidates for suppressors of the early flowering phenotype of *lhp1* are, apart from mutations in *FT*, mutations in the autonomous pathway. Autonomous pathway mutations result in a strong up-regulation of the floral repressor *FLOWERING LOCUS C* (*FLC*) that directly targets and represses *FT* (Simpson, 2004; Searle et al., 2006; Jiang et al., 2008). *FLC* levels are also moderately increased in the PcG pathway mutants *curly leaf* (*clf*) and *lhp1* (Mylne et al., 2006; Jiang et al., 2008). However, this moderate increase is not able to suppress *FT* up-regulation caused by the loss of PcG mediated repression (Kotake et al., 2003; Farrona et al., 2011). *FLC* levels were not dramatically increased and *FT* levels were not significantly altered between *alp1;lhp1* and *lhp1* compared to other suppressor mutations that were likely to be affected in the autonomous pathway (Supplemental Fig. S1). In contrast to *alp1;lhp1* plants, the leaf size is not increased in *ft;lhp1* double mutants, which made it also unlikely that the suppression was caused by a mutation in *FT*. No differences in flower morphology could be observed when flowers of *lhp1* and the double mutant were compared to each other (Supplemental Fig. S2).

The pleiotropic phenotype of *lhp1* mutant plants differs quantitatively between accessions such as Col-0 and Ws-2 making it difficult to create a robust mapping population for subtle modifiers (Supplemental Fig. S3). Progeny of a *alp1*;*lhp1* cross to the original *lhp1* allele segregated with a 3:1 ratio for the suppressor phenotype in the F_2 generation indicating that a single mutation was responsible for the suppression. One of the F_2 plants with a suppressor phenotype was randomly picked and backcrossed a second time to *lhp1* and gave rise to another F_2 generation (BC_2F_2).

Fast isogenic mapping-by-sequencing reveals candidate mutations

Leaf samples of 270 BC_2F_2 *alp1*;*lhp1* plants were pooled. DNA prepared from the pooled material was sequenced on a single lane of an Illumina Genome Analyzer IIx. In parallel, DNA of 48 pooled *lhp1* single mutant leaves from the parental line was sequenced as reference on a separate sequencing reaction. The parental line had been generated from an EMS mutagenesis in the background of Col-0 and had been backcrossed to the parental Col-0 for an unknown number of times (Larsson et al., 1998).

Out of 43.4 and 42.2 million high quality reads, 93% and 94% aligned to the reference sequence and yielded an average nucleic genome coverage of 41- and 49-fold for *lhp1* and *alp1*;*lhp1*, respectively (Supplemental Table 1). Differences between the reference sequence and both sequence sets were independently identified with SHORE (Ossowski et al., 2008; Materials and Methods). Within the resequencing data of the BC_2F_2 *alp1*;*lhp1*, short read analysis was performed to identify all mutations with an allele frequency higher than 20%, in order to identify fixed as well as non-fixed EMS mutations segregating in the pool (Materials and Methods). By removing all sequence differences that had their origin in the *lhp1* genome from the *alp1*;*lhp1* sequence we defined a set of 852 novel EMS changes (G/C:A/T) that were specific for the BC_2F_2 *alp1*;*lhp1* pool.

Using SHOREmap to visualize the allele frequency estimations at the mutant loci, selection for the lower arm of chromosome 3 became apparent through an allele frequency distortion in this region (Fig. 3, Materials and Methods). Out of three EMS mutations that had a mutant allele frequency higher than 80%, two were found to be located in exons of At3g57940 and At3g63270 and one in an intron of At3g61130. The first two mutations caused missense mutations leading to amino acid changes of V-I and G-E, respectively (Fig. 4, Supplemental Table 2).

Deep candidate resequencing (dCARE) identifies causal change

Near to complete linkage between the three candidate mutations was apparent in the pooled DNA, even though the mutations were spaced over 2 Mbp apart. Based on Arabidopsis genetic maps this physical distance corresponds to approximately 7-8 cM suggesting that several recombination events between these mutations are expected in a pool of 270 recombinants (Giraut et al., 2011). Our analysis of the raw reads covering the three mutations revealed two Col-0 WT reads for the mutation in At3g57940, as well as for the intronic change in At3G61130, but only one WT read for the mutation in At3g63270 (Supplemental

Table 3). Although the mutation in At3g63270 could therefore act as main candidate the disparity was too minor to reliably exclude the other mutations. This is a sampling problem as usually the number of individuals pooled in bulk segregant analyses is considerably larger than the read coverage, which is therefore not powerful enough to resolve the real allele frequency accurately. However, an increased number of short read alignments at the mutations would help to resolve the real allele frequency of the mutant allele in the bulked DNA much more precisely (Fig. S4). In order to generate more sequencing data for the mutated regions, we amplified regions across the mutations by PCR using the pooled DNA from bulked segregants as template and sequenced the amplicons with the Ion Torrent Personal Genome Machine (PGM) (Rothberg et al., 2011). This deep candidate resequencing (or dCARE) analysis generated 20,111, 4,390 and 19,203 reads across the changes affecting At3g57940, At3g61130 and At3g63270, respectively. For the changes in At3g57940 and At3g61130 we found 5.7% and 2.1% reads not supporting the mutant allele, whereas only 0.45% of the reads at At3g63270 supported the wild-type allele.

The presence of Col-0 WT reads at all candidate mutations can be explained by contamination of the segregant bulk, possibly due to misscoring of mutants or by sequencing errors that occur at a low rate. Both types of error affect mutations independently of their linkage to the causative change and represent a background noise. In fact, the rate of non-mutant alleles at At3g63270 is even slightly lower than the rate of sequencing errors reported for Ion Torrent PGM sequencing (Rothberg et al., 2011). As a consequence we could not reliably identify any WT alleles for the mutation affecting At3g63270, whereas the WT allele was clearly apparent for both linked mutations (Supplemental Table 3). Thus, dCARE reduced the list of candidates to At3g63270.

Validation of mutation causing the phenotype

A second suppressor mutant of *lhp1*, also identified in our forward genetic screen, displayed a phenotype similar to the *alp1*;*lhp1* double mutant. Reciprocal crosses between the two suppressor mutants showed that they were likely allelic to each other, since all F_1 individuals of reciprocal crosses looked as *alp1;lhp1* (Fig. 5A). The three candidate loci analyzed by dCARE were sequenced in the second suppressor and in a single *alp1*;*lhp1* M3 plant. We could confirm all mutations in *alp1;lhp1*, but in the second suppressor only At3g63270 was disrupted by a G to A change leading to a premature stop codon (Fig. 5B). We designated the allele underlying the original suppressor mutation as *alp1-1*, the allele with the internal stop codon as *alp1-2*. A third allele, *alp1-3*, was caused by a T-DNA insertion from an enhancer

trap line that disrupted the third exon of *ALP1* (ET1398, http://genetrap.cshl.edu). The *alp1-3* allele was in the L*er* backround and the F2 generation from a cross between *alp1-3* and *lhp1* showed a range of suppression phenotypes of *lhp1*. We therefore scored three F_3 families that were homozygous for *alp1-3;lhp1* and compared their flowering time with that of *lhp1* and WT Col-0 (Figure 5C and D). The data confirmed that *alp1-3* suppressed the early flowering of *lhp1* and increased the leaf size to a value that was intermediate between *lhp1* and WT Col-0.

ALP1 is related to *Harbinger*-like transposases

ALP1 encodes a gene related to *Harbinger*-like transposases. *Harbinger* transposases belong to the P instability factor or (*PIF*) superfamily of transposases and code for a transposase as well as an accessory protein with a potential DNA binding Myb/SANT domain. In particular, *ALP1* encodes the transposase component, which features an endonuclease domain of the DDE-4 superfamily (PSSM id cl15789, e-value: 3.54e-19 in NCBI Conserved Domain Database (CDD) search) (Marchler-Bauer et al., 2011). These endonucleases contain a catalytic triad if three acidic amno-acid residues (DDE) that coordinate metal ions needed for catalysis (Yuan and Wessler, 2011). An amino-terminal helix-turn-helix (HTH) between amino acids 110 and 141 of ALP1 is supported by NCBI CDD (PSSM id cl00088, e-value 5.05e-3).

To evaluate if ALP1 was an active transposon showing expansion in the Arabidopsis genome, we compared ALP1 to its closest homologues available from a GenBank BLAST search using unique protein sequences from all species. ClustalW sequence alignment and calculation of a neighbor-joining tree showed that ALP1 amino acid sequence did not cluster together with the seven other *Harbinger*-like genes from *Arabidopsis* or with an out-group of functional *Harbinger*-related transposases such as IS5 from bacteria (Fig. 6). The *ALP1* clade included four additional plant proteins of unknown function from soybean, poplar, grapewine and castor bean whereas the closest Arabidopsis homologue, At3g55350, was present in a distinct branch of the tree. The data show that ALP1 is encoded by a single copy gene in Arabidopsis and is found in different plant families. Notably, the HTH domain, which could represent a DNA-binding motif, was shared within the ALP1 clade but was not detected in any of the other Arabidopsis homologues of ALP1 by a CCD search.

The alignment of the ALP1 clade with At3g55350 and HARBI1 from humans and zebra fish, provided evidence that the acidic triad with the conserved amino residues “DDE” is disrupted in all members of the ALP1 clade (Supplemental Fig. S5). As the DDE triad is

required for catalysis it is likely that members of the ALP1 clade have lost their endonuclease activity.

ALP1 is an expressed gene that is not directly regulated by LHP1 and the PcG pathway (Supplemental Fig. S6A and B). Expression levels were not altered in *lhp1* seedlings compared to WT and the epigenetic landscape of *ALP1* was free of H3K27me3 and LHP1 (Zhang et al., 2007; Farrona et al., 2011).

Thus, we hypothesize that *ALP1* is derived from an ancient Harbinger transposon, but seems to have acquired a plant specific function over time.

Discussion

Conventional genetic mapping requires outcrossing to a diverged accession for establishment of a mapping population. However, differences in phenotypes that segregate between Arabidopsis accessions are likely to mask subtle phenotypes caused by mutations. We have by-passed this problem by backcrossing an EMS-induced double mutant plant to its single mutant parent generating an isogenic mapping population. Consequently, conventional markers are absent in the population and cannot be used to distinguish parental alleles. However, as we performed whole-genome sequencing it was possible to identify mutagen-induced changes and to use them as markers as these are only specific to the mutant genome and are absent in the original genome. This allowed scoring of a mapping population for the mutant phenotype only using the original genetic background. This method opens possibilities for the identification of subtle phenotypes that were previously inaccessible.

In addition, fast isogenic mapping-by-sequencing saves a large amount of time and labor needed in comparison to classical mapping approaches (Abe et al., 2012). After sequencing, data analysis to produce putative candidate genes will take only a day using automated pipelines, like the one provided for download with this report (http://shoremap.org).

Whole-genome sequencing of pooled DNA from bulked segregants usually does not allow for a unique identification of the causal change, but results in a list of linked candidate changes. Mutations, which are closely linked with the causal mutation, are only influenced by a minor number of recombination and the coverage of whole genome resequencing does not allow distinguishing between homozygous and near homozygous changes. If the complement of pooled segregants is likely to introduce a low rate of recombination between closely linked candidate mutations, non-causative mutations can be excluded by a quantitative detection of rare WT alleles. Introducing dCARE to the mapping pipeline allowed us to drastically

increase the coverage for linked changes, which reduced the list of candidates to one (causal) change, with comparably little additional effort.

The number of segregants required to unambiguously identify a single mutation as the main candidate depends on various factors including EMS-load, recombination frequency and the error rate in scoring the phenotype. The detected load of EMS mutation in *alp1;lhp1* was low and helped in reducing the number of candidate genes to three, but the dCARE could have been easily extended to more sequence differences at very low additional cost. A low mutation rate harbors other drawbacks as it reduces the number of mutants identified in an EMS screen. In particular, the availability of a second allele with the same phenotype from the screen proved to be a big advantage in confirming the resequencing results (Fig. 5).

ALP1 is related to type II dsDNA transposases, which are the most abundant and possibly most essential elements for evolution in viral, bacterial and eukaryotic genomes (Aziz et al., 2010). They can fulfill essential functions for an organism, such as DNA processing (Landweber et al., 2009). The catalytic acidic triad “DDE” that was found to be disrupted in ALP1 is characteristic of the transposase/integrase supergroup and is essential in coordinating metal ions involved in the “cut and paste” mechanism of dsDNA transposases (Yuan and Wessler, 2011, Craig, 2002; Casola et al., 2007). The fact that functional relevant amino acid residues were not conserved in the ALP1 protein supports our hypothesis that the protein does not function as an active transposase. Of seven homologues of ALP1 in Arabidopsis, four clustered together with active transposases in bacteria in a neighbour-joining analysis, whereas the others were present in distinct clades of the tree. These clades contained only plant proteins from other species, suggesting coexistence between active and inactive *Harbingers* in Arabidopsis (Fig. 6). *ALP1* might be able to bind DNA through one or two helix-turn-helix motifs towards the amino-terminal end of the protein (Iwahara et al., 1998). This function could be exclusive for the ALP1 clade, since a CDD search did not detect the same domain structure in the other Arabidopsis homologues.

In conclusion, *ALP1* is an actively transcribed gene that is related to Harbinger transposases but likely to have lost its ability to transpose. To reveal the function of ALP1 in detail and in particular elucidate its interaction with the *lhp1* mutation remains a challenging task for the future.

Materials and Methods

Treatment of seeds

Germination rates of *lhp1* and WT seeds were scored on GM plates after 10 LDs at 22°C in a Percival plant growth chamber (CLF Plant Climatics, Wertingen, Germany). For EMS treatment 200 mg of seeds were wrapped into miracloth and imbibed on a shaker at 4°C in 0.1 % KCl solution for 14 h. Seeds were then washed with distilled water and treated with 100 ml of 30mM EMS diluted in distilled water on a magnetic stirrer for 12 h.

Two washing steps with 100 ml of 100 mM sodium thiosulfate for 15 min and three washing steps with 500 ml dH_2O for 30 min followed. After washing, seeds were equally divided into five bottles containing 500 ml of 0.1 % Universal Agarose (Bio-Budget Technologies GmbH, Krefeld, Germany). Seeds were sown in 7.5 ml aliquots onto 9×9 cm pots using plastic pipettes.

Selection of potential mutants

M1 plants were bagged in small bulks averaging three plants. For each M1 plant 10 M2 seeds were sown onto 9×9 cm pots in four rows of five plants each. Potential mutants were primarily screened in short day (SD) conditions and grown together with *lhp1* (Col-0) also termed *tfl2-2* (Larsson et al., 1998), *lhp1*;*clf* (Salk 006658) (Col-0), *lhp1* (Col-0);*emf2-10* (Ws-2, Chanvivattana et al., 2004) mutants and Col-0 WT plants as controls.

Bulks with potential mutants were re-screened in a Percival chamber at 60% humidity, 12 h light, 16 °C day and 14 °C night temperature. At least ten plants of each potential mutant were grown in the M3 at the same conditions to confirm stability of the previously recorded phenotype. Randomly selected M3 plants scored as confirmed mutants were backcrossed to Col-0 and *lhp1* to generate BC_1F_1 seeds. For the Col-0 backcross, the following BC_1F_2 generation was also scored for absence or presence of additional segregating phenotypes. Stability and segregation rate of the mutant phenotype was scored in the *lhp1* backcross. One randomly selected BC_1F_2 *alp1-1;lhp1* plant was again backcrossed to *lhp1* to generate a BC_2F_2 population.

Flowering time measurements

Seeds were stratified for 3 days at 4°C on soil in the dark and transferred either to Percival plant growth chambers (CLF Plant Climatics, Wertingen, Germany) set to LD conditions (16h light/22°C, 8h dark/20°C) or set to screening LD conditions (12h light/16°C, 12h dark/14°C). Rosette and cauline leaves were counted as measure for flowering time. Statistical significance was evaluated by single factor ANOVA followed by an honesty significant difference Tukey test. Letters above bars indicate significantly different groups ($p<0.05$)

Library preparation and sequencing

Approximately 1,000 BC_2F_2 plants were sown and leaf samples of equal size were collected from 270 plants scored as *alp1-1;lhp1*. In parallel, leaf samples were collected from 48 *lhp1* plants. The leaves were bulked prior to DNA extraction with DNeasy® Plant Maxi Kit (Qiagen, Hilden, Germany). DNA was eluted with 500 µl H_2O in four steps. DNA concentration and quality was determined with a Nanodrop 1000 (Peqlab, Erlangen, Germany) and on a 1% agarose gel. DNA samples were concentrated to more than 50 ng × μl^{-1} with a speed-vac when necessary.

Samples of more than 3µg of total high-quality DNA extract (260/280 ratio > 1,8) were sequenced by the Cologne Center for Genomics (CCG, Köln, Germany). At the CCG a quality check of the samples was performed with a bioanalyzer (Agilent 2100, Agilent, Böblingen, Germany). Libraries were generated using the Illumina Genomic DNA sample kit (Illumina, San Diego, CA) according to the manufacturer's instruction. DNA concentration of the amplified libraries was measured with the DNA 1000 kit as well as the DNA high sensitivity kit for diluted libraries (both Agilent). The samples were sequenced on an Illumina Genome Analyzer GAIIx in a 96 bp paired end run.

Resequencing analysis

We applied SHORE to independently align the read sets of the *lhp1* mutant and the *alp1-1;lhp1* double mutant to the Col-0 reference genome using GenomeMapper as alignment tool (Ossowski et al., 2008; Schneeberger et al., 2009; Schneeberger et al., 2009;ArabidopsisGenomeConsortium;TAIR10). Using the function SHORE *import*, raw reads were trimmed or discarded based on quality values with a cut-off Phred score +38. After correcting the paired-end alignments with an expected insert size of 300 bp, we applied SHORE *consensus* to identify variations between the mutants and reference. We removed background of *alp1;lhp1* by filtering out all the difference between *lhp1* and the reference sequence from *alp1;lhp1*. *alp1;lhp1*-specific canonical EMS changes with high quality (SHORE score > 24) and supported by more than seven reads, were used in SHOREmap *backcross* for allele frequency analysis. Allele frequencies estimates were calculated as the ratio of the reads of mutant allele divided by all reads at a particular locus. Sequence changes in the region that featured evidence for selection were annotated for their effect on gene identity using TAIR10 gene annotation. See Supplemental Table 4 for command line calls for the resequencing and mapping-by-sequencing.

dCARE

Primers for dCARE were designed with the help of Primer3 (v. 0.4.0) to amplify 80-150 bp amplicons that contained the candidate mutations at a distance from +1 to +50 from the 3'end of the primer that contained the A-type extension required for Ion Torrent PGM sequencing (Primers are listed in Supplemental Table 5). DNA was amplified from the same pool of DNA as used for whole genome resequencing. Amplicons were purified using Agencourt® AMPure® beads (Beckmann Coulter GmbH, Krefeld, Germany) according to the manufacturer's instruction. Amplicons were quantified by OD260, pooled with samples from other customers and sequenced in an Ion Torrent PGM (Life Technologies, Guilford, CT, USA) using a 316K chip to a depth of 5.000 - 20.000 reads per amplicon.

Allele frequencies of both wild type and mutant were estimated from raw reads. Using a 21-mer around the mutation site, an ad-hoc script was used to count the allele occurrence with perfect or one mismatch. Coverage at each locus was calculated by the sum of satisfying reads from the above criteria.

Quantification of mRNA abundance

After the removal of roots, total RNA was extracted from the aerial part of 10d old seedlings grown on soil or on GM plates with an RNeasy® Plant Mini kit (Qiagen, Hilden, Germany) according to the manufacturer's instructions. 1 µg RNA of each sample was loaded onto a 1% Agarose gel to control for RNA degradation by visualizing the two distinct rRNA bands.

When quality control was passed 5 µg of RNA was treated with DNase I using a DNA-free™ kit (Ambion, Life Technologies, Guilford, CT, USA). After DNase treatment cDNA was synthesized with a dT18 primer and a Superscript II reverse transcriptase kit (Invitrogen, Life Technologies, CT, USA) according to the manufacturer's instructions. Samples were diluted to 150 µl with dH_2O and 1-3 µl of cDNA was used for qRT-PCR. All qRT-PCRs were performed in a BioRAD iCycler iQ5™ with EvaGreen® (Biotium, Hayward, CA, USA) as a chelating fluorescent dye to quantify the real-time signal. Primers used for the quantification of mRNA are listed in Supplemental Table S5.

Neighbour-joining analysis

Amino acid sequences were aligned using clustalW implemented in MEGA5 (Tamura et al., 2011). The analysis involved 105 amino acid sequences that were identified by BLAST against non-redundant proteins in the NCBI database. The evolutionary history was inferred

using the neighbor-joining method (Saitou and Nei, 1987). The bootstrap consensus tree inferred from 10,000 replicates was taken to represent the evolutionary history of the taxa analyzed (Felsenstein, 1985). Branches showing partitions reproduced in less than 50% bootstrap replicates are collapsed. The evolutionary distances were computed using the number of differences method (Nei and Kumar, 2000) and are in the units of the number of base differences per sequence. There were a total of 3,082 positions in the final dataset. Evolutionary analyses were conducted in MEGA5 (Tamura et al., 2011).

Acknowledgement

The author would like to thank Mitzi Villajuana-Bonequi for helpful discussions on EMS mutagenesis and Dr. Mbaye Tine for help with Ion Torrent sequencing.

References

Abe A, Kosugi S, Yoshida K, Natsume S, Takagi H, Kanzaki H, Matsumura H, Mitsuoka C, Tamiru M, Innan H, Cano L, Kamoun S, Terauchi R (2012) Genome sequencing reveals agronomically important loci in rice using MutMap. Nat Biotechnol **30:** 174-178

Alonso AGD, Gutierrez L, Fritsch C, Papp B, Beuchle D, Muller J (2007) A genetic screen identifies novel polycomb group genes in Drosophila. Genetics **176:** 2099-2108

Ashelford K, Eriksson ME, Allen CM, D'Amore R, Johansson M, Gould P, Kay S, Millar AJ, Hall N, Hall A (2011) Full genome re-sequencing reveals a novel circadian clock mutation in Arabidopsis. Genome Biol **12:**R28

Austin RS, Vidaurre D, Stamatiou G, Breit R, Provart NJ, Bonetta D, Zhang JF, Fung P, Gong YC, Wang PW, McCourt P, Guttman DS (2011) Next-generation mapping of Arabidopsis genes. Plant Journal **67:** 715-725

Aziz RK, Breitbart M, Edwards RA (2010) Transposases are the most abundant, most ubiquitous genes in nature. Nucleic Acids Res **38:** 4207-4217

Bratzel F, Lopez-Torrejon G, Koch M, Del Pozo JC, Calonje M (2010) Keeping cell identity in arabidopsis requires PRC1 RING-finger homologs that catalyze H2A monoubiquitination. Curr Biol **20:** 1853-1859

Casola C, Lawing AM, Betran E, Feschotte C (2007) PIF-like Transposons are common in Drosophila and have been repeatedly domesticated to generate new host genes. Molecular Biology and Evolution **24:** 1872-1888

Chanvivattana Y, Bishopp A, Schubert D, Stock C, Moon YH, Sung ZR, Goodrich J (2004) Interaction of polycomb-group proteins controlling flowering in Arabidopsis. Development **131:** 5263-5276

Craig NL (2002) Mobile DNA II. ASM Press, Washington, D.C.

Cuperus JT, Montgomery TA, Fahlgren N, Burke RT, Townsend T, Sullivan CM, Carrington JC (2010) Identification of MIR390a precursor processing-defective mutants in Arabidopsis by direct genome sequencing. Proceedings of the National Academy of Sciences of the United States of America **107:** 466-471

Exner V, Aichinger E, Shu H, Wildhaber T, Alfarano P, Caflisch A, Gruissem W, Kohler C, Hennig L (2009) The chromodomain of LIKE HETEROCHROMATIN PROTEIN 1 is essential for H3K27me3 binding and function during Arabidopsis development. PLoS ONE **4:** e5335

Farrona S, Thorpe FL, Engelhorn J, Adrian J, Dong X, Sarid-Krebs L, Goodrich J, Turck F (2011) Tissue-Specific Expression of FLOWERING LOCUS T in Arabidopsis Is Maintained Independently of Polycomb Group Protein Repression. Plant Cell **23:** 3204-3214

Felsenstein J (1985) Confidence-Limits on Phylogenies - an Approach Using the Bootstrap. Evolution **39:** 783-791

Gildea JJ, Lopez R, Shearn A (2000) A screen for new trithorax group genes identified little imaginal discs, the Drosophila melanogaster homologue of human retinoblastoma binding protein 2. Genetics **156:** 645-663

Giraut L, Falque M, Drouaud J, Pereira L, Martin OC, Mezard C (2011) Genome-Wide Crossover Distribution in Arabidopsis thaliana Meiosis Reveals Sex-Specific Patterns along Chromosomes. Plos Genetics **7**

Iwahara J, Kigawa T, Kitagawa K, Masumoto H, Okazaki T, Yokoyama S (1998) A helix-turn-helix structure unit in human centromere protein B (CENP-B). Embo Journal **17:** 827-837

Jiang D, Wang Y, He Y (2008) Repression of FLOWERING LOCUS C and FLOWERING LOCUS T by the Arabidopsis Polycomb repressive complex 2 components. PLoS ONE **3:** e3404

Kotake T, Takada S, Nakahigashi K, Ohto M, Goto K (2003) Arabidopsis TERMINAL FLOWER 2 gene encodes a heterochromatin protein 1 homolog and represses both FLOWERING LOCUS T to regulate flowering time and several floral homeotic genes. Plant Cell Physiol **44:** 555-564

Landecker HL, Sinclair DAR, Brock HW (1994) Screen for Enhancers of Polycomb and Polycomblike in Drosophila-Melanogaster. Developmental Genetics **15:** 425-434

Landweber LF, Nowacki M, Higgins BP, Maquilan GM, Swart EC, Doak TG (2009) A Functional Role for Transposases in a Large Eukaryotic Genome. Science **324:** 935-938

Larsson AS, Landberg K, Meeks-Wagner DR (1998) The TERMINAL FLOWER2 (TFL2) gene controls the reproductive transition and meristem identity in Arabidopsis thaliana. Genetics **149:** 597-605

Makarevich G, Leroy O, Akinci U, Schubert D, Clarenz O, Goodrich J, Grossniklaus U, Kohler C (2006) Different Polycomb group complexes regulate common target genes in Arabidopsis. Embo Reports **7:** 947-952

Marchler-Bauer A, Lu SN, Anderson JB, Chitsaz F, Derbyshire MK, DeWeese-Scott C, Fong JH, Geer LY, Geer RC, Gonzales NR, Gwadz M, Hurwitz DI, Jackson JD, Ke ZX, Lanczycki CJ, Lu F, Marchler GH, Mullokandov M, Omelchenko MV, Robertson CL, Song JS, Thanki N, Yamashita RA, Zhang DC, Zhang NG, Zheng CJ, Bryant SH (2011) CDD: a Conserved Domain Database for the functional annotation of proteins. Nucleic Acids Res **39:** D225-D229

Mylne JS, Barrett L, Tessadori F, Mesnage S, Johnson L, Bernatavichute YV, Jacobsen SE, Fransz P, Dean C (2006) LHP1, the Arabidopsis homologue of HETEROCHROMATIN PROTEIN1, is required for epigenetic silencing of FLC. Proc Natl Acad Sci U S A **103:** 5012-5017

Nei M, Kumar S (2000) Molecular evolution and phylogenetics. Oxford University Press, Oxford ; New York

Ossowski S, Schneeberger K, Clark RM, Lanz C, Warthmann N, Weigel D (2008) Sequencing of natural strains of Arabidopsis thaliana with short reads. Genome Research **18:** 2024-2033

Page DR, Grossniklaus L (2002) The art and design of genetic screens: Arabidopsis thaliana. Nature Reviews Genetics **3:** 124-136

Rothberg JM, Hinz W, Rearick TM, Schultz J, Mileski W, Davey M, Leamon JH, Johnson K, Milgrew MJ, Edwards M, Hoon J, Simons JF, Marran D, Myers JW, Davidson JF, Branting A, Nobile JR, Puc BP, Light D, Clark TA, Huber M, Branciforte JT, Stoner IB, Cawley SE, Lyons M, Fu YT, Homer N, Sedova M, Miao X, Reed B, Sabina J, Feierstein E, Schorn M, Alanjary M, Dimalanta E, Dressman D, Kasinskas R, Sokolsky T, Fidanza JA, Namsaraev E, McKernan KJ, Williams A, Roth GT, Bustillo J (2011) An integrated semiconductor device enabling non-optical genome sequencing. Nature **475:** 348-352

Saitou N, Nei M (1987) The Neighbor-Joining Method - a New Method for Reconstructing Phylogenetic Trees. Molecular Biology and Evolution **4:** 406-425

Schneeberger K, Hagmann J, Ossowski S, Warthmann N, Gesing S, Kohlbacher O, Weigel D (2009) Simultaneous alignment of short reads against multiple genomes. Genome Biol **10:** R98

Schneeberger K, Ossowski S, Lanz C, Juul T, Petersen AH, Nielsen KL, Jorgensen JE, Weigel D, Andersen SU (2009) SHOREmap: simultaneous mapping and mutation identification by deep sequencing. Nat Methods **6:** 550-551

Searle I, He YH, Turck F, Vincent C, Fornara F, Krober S, Amasino RA, Coupland G (2006) The transcription factor FLC confers a flowering response to vernalization by repressing meristem competence and systemic signaling in Arabidopsis. Genes & Development **20:** 898-912

Simpson GG (2004) The autonomous pathway: epigenetic and post-transcriptional gene regulation in the control of Arabidopsis flowering time. Curr Opin Plant Biol **7:** 570-574

Tamura K, Peterson D, Peterson N, Stecher G, Nei M, Kumar S (2011) MEGA5: Molecular Evolutionary Genetics Analysis Using Maximum Likelihood, Evolutionary Distance, and Maximum Parsimony Methods. Molecular Biology and Evolution **28:** 2731-2739

Turck F, Roudier F, Farrona S, Martin-Magniette ML, Guillaume E, Buisine N, Gagnot S, Martienssen RA, Coupland G, Colot V (2007) Arabidopsis TFL2/LHP1 specifically associates with genes marked by trimethylation of histone H3 lysine 27. Plos Genetics **3:** 855-866

Xu L, Shen WH (2008) Polycomb silencing of KNOX genes confines shoot stem cell niches in Arabidopsis. Curr Biol **18:** 1966-1971

Yuan YW, Wessler SR (2011) The catalytic domain of all eukaryotic cut-and-paste transposase superfamilies. Proc Natl Acad Sci U S A **108:** 7884-7889

Zhang X, Germann S, Blus BJ, Khorasanizadeh S, Gaudin V, Jacobsen SE (2007) The Arabidopsis LHP1 protein colocalizes with histone H3 Lys27 trimethylation. Nature Structural & Molecular Biology **14:** 869-871

Figure legends

Figure 1: Schematic illustration of fast isogenic mapping approach.

Chemical mutagens typically introduce hundreds of novel mutations. Within the M2 generation, mutants are screened for phenotypes. Selected plants are backcrossed to the non-mutagenized progenitor. The F_2 offspring of such a cross forms an isogenic mapping population as only novel mutations are segregating. Backcrossed individuals that display the mutant phenotype are selected, bulked, their DNA is prepared as a pool and whole-genome sequenced. If the parental line is genetically different from the reference line Col-0, it needs to be resequenced in order to control for naturally occurring differences that need to be differentiated from novel mutations. Thus, all novel EMS-induced mutations can be selected for SHOREmap analysis by filtering for mutations that do not reside in the parental line. Candidate mutations (see gray box) that show high mutant allele frequencies and linkage are selected for deep candidate resequencing (dCARE) to pinpoint the causal mutation.

Figure 2: Phenotype comparisons.

(**A-C**) Col-0 WT, *alp1;lhp1* double and *lhp1* single mutants 36 days after germination and growth in climate chamber conditions (12h light/16 °C, 12h dark/14 °C). One representative example for each genotype is shown as (**A**) whole plant, (**B**) the 3rd oldest cauline leaf of the main shoot and (**C**) the 7th youngest silique of the main shoot. White bars represent 1 cm. (**D**) Flowering time analysis. Plants grown as in (A-C) were scored when the main shoot had bolted to about 1 cm height. The leaf number is indicated on the y-axis. Error bars represent the standard error of the mean (n=9). Statistical significance was evaluated by single factor ANOVA followed by an honesty significant difference Tukey test. Letters above bars indicate significantly different groups ($p<0.05$).

Figure 3: Allele frequency estimations at EMS changes. Allele frequency estimations at EMS-induced mutations of *alp1*;*lhp1* across all 5 chromosomes (Mb, x-axis). Allele frequencies (AF, y-axis) were estimated as fraction of short reads supporting the mutant allele divided by the number of all reads aligning to a given marker. The color indicates the resequencing consensus (SHORE) score, only base calls with a quality score of more than 25 have been considered. The long arm of chromosome 3 was found to be under selection, as local allele frequencies appeared higher as compared to other regions in the genome.

Figure 4: Annotation of putative causal mutations.

The genomic regions of candidate EMS mutations (red asterisks) along with gene annotations are shown. Orange boxes indicate exons. Locations of EMS mutations that have putative effects on amino acid sequences are shown in red letters; for clarity the DNA sequences in the graph do not reflect the actual number of reads at these locations (coverage was 50-fold).

Figure 5: Validation of the causal mutation.

(**A**) Complementation test of two EMS induced alleles of *alp1*. F1 progeny from reciprocal crosses of two suppressors of *lhp1* with similar phenotypes (*alp1-1;lhp1* and *alp1-2;lhp1).* Single *lhp1* mutants are shown as reference as indicated. (**B**) EMS induced changes at *ALP1* and point of T-DNA insertion of *alp1-3*. In addition to the mutations identified in *alp1-1;lhp1* by whole-genome sequencing, a point mutation leading to a premature stop codon was found in *alp1-2;lhp1*. Arrows indicate position of PCR primers used for dCARE. (**C**, **D**) Analysis of T-DNA insertion allele *alp1-3* (**C**) Representatives of three double homozygous F3 families

derived from the cross of *alp1-3* with *lhp1*. (**D**) Flowering time measurements in three double homozygous *alp1-3;lhp1* F3 families as in (C). Plants were grown in LD in Percival cabinet conditions (16h light/22°C, 8h dark/20°C). Y-axis shows leaf number until bolting for rosette and cauline leaves. Error bars represent the standard error of the mean. Statistical significance was evaluated by single factor ANOVA followed by an honesty significant difference Tukey test. Letters above bars indicate significantly different groups ($p<0.05$).

Figure 6: Phlyogenetic analysis of ALP1.

Nine of the twelve subclades of the neighbor-joining tree have been collapsed to emphasize the ALP1 (VII), At3g55350 (II) and IS5 (XI) subclades. The number of proteins within collapsed clades is indicated in brackets. The tree is drawn with branch lengths linear to the evolutionary distances used to infer the phylogenetic tree. Four unknown proteins from different plant species cluster with ALP1 in subclade VI. ALP1 and its closest homologue At3g55350 were assigned to two distinct clades. The XI outgroup contains active transposons from bacteria and plants, four of the seven ALP1 Arabidopsis homologues and an additional Arabidopsis protein that is most closely related to the transposase encoded by *ATIS112A,* an annotated Harbinger transposon from Arabidopsis. Clade XII contains 48 proteins from plants and animals, including the human HARB1 protein.

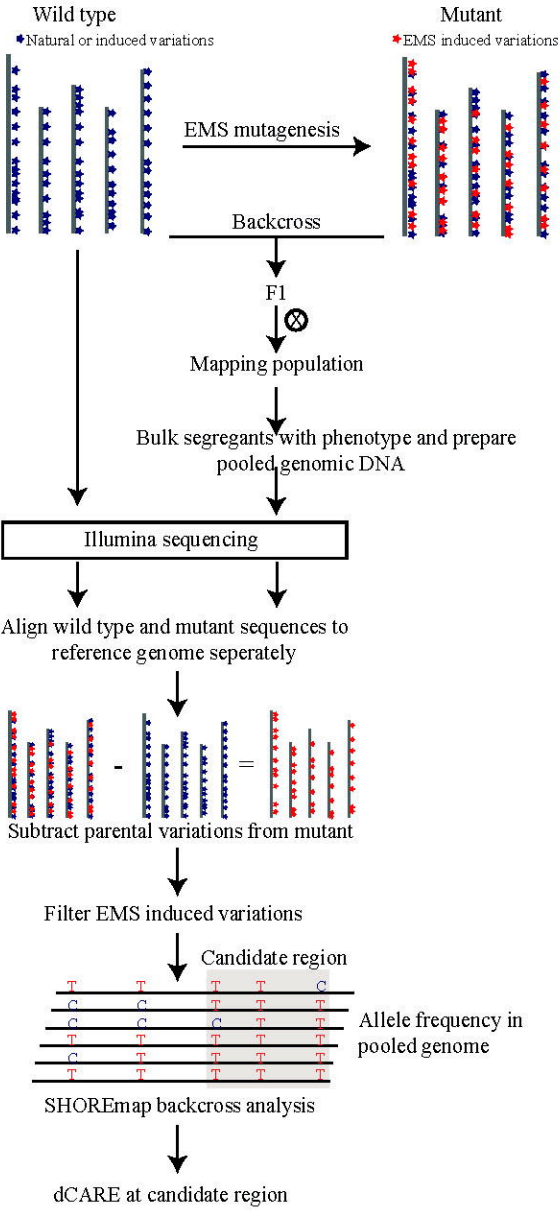
Wild type
Natural or induced variations
Mutant
EMS induced variations
EMS mutagenesis
Backcross
F1
Mapping population
Bulk segregants with phenotype and prepare pooled genomic DNA
Illumina sequencing
Align wild type and mutant sequences to reference genome seperately
Subtract parental variations from mutant
Filter EMS induced variations
Candidate region
Allele frequency in pooled genome
SHOREmap backcross analysis
dCARE at candidate region

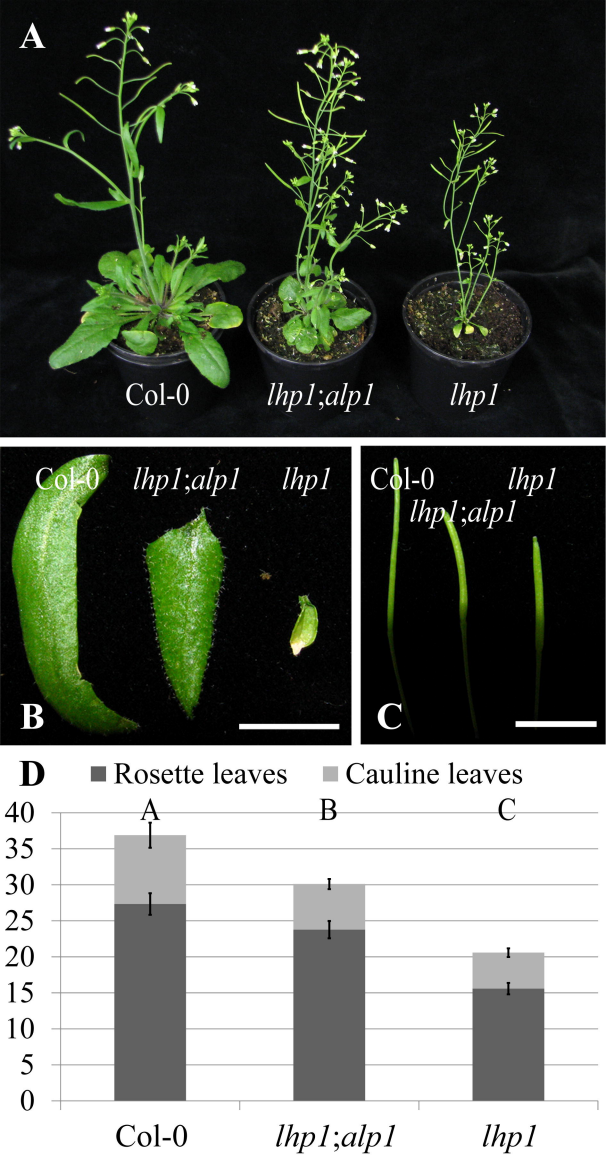
A
Col-0
lhp1;alp1
lhp1
B
Col-0
lhp1;alp1
lhp1
C
Col-0
lhp1
lhp1;alp1
D
Rosette leaves
Cauline leaves
A
B
C
40
35
30
25
20
15
10
5
0
Col-0
lhp1;alp1
lhp1

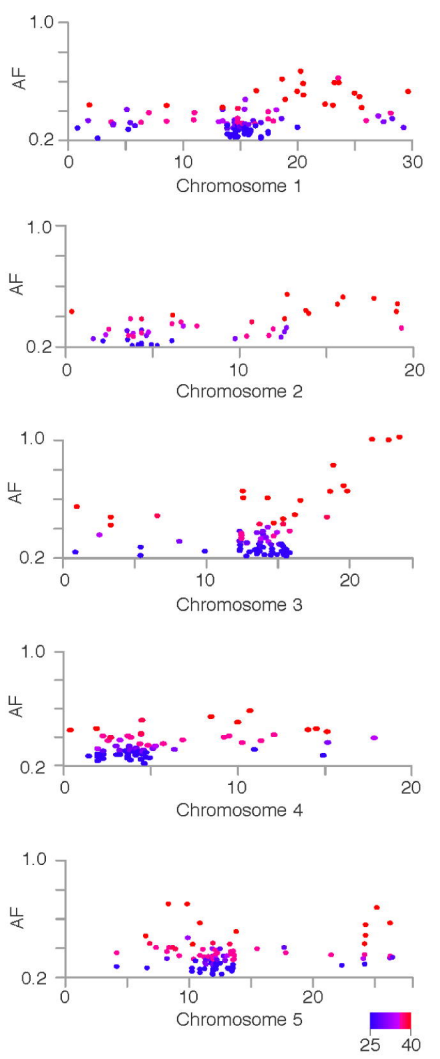
1.0
AF
0.2
0
10
20
30
Chromosome 1
1.0
AF
0.2
0
10
20
Chromosome 2
1.0
AF
0.2
0
10
20
Chromosome 3
1.0
AF
0.2
0
10
20
Chromosome 4
1.0
AF
0.2
0
10
20
Chromosome 5
25
40

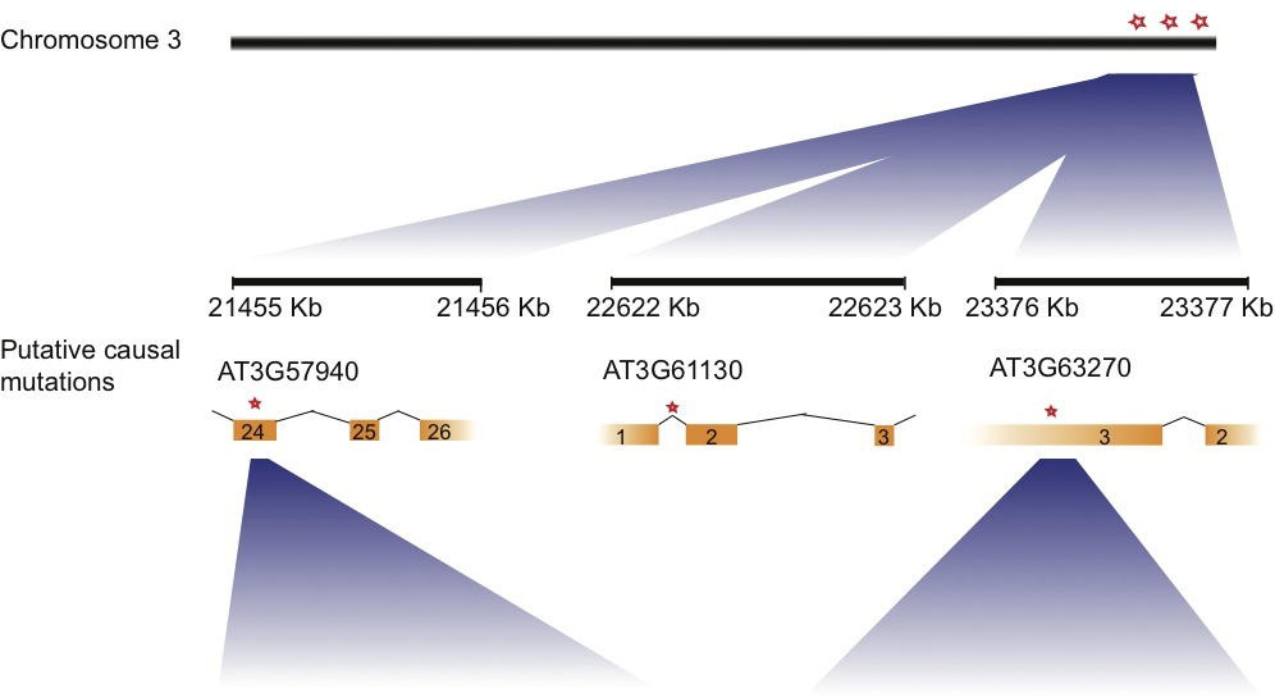

DNA sequence

TCTCTTCTCCTGAAGGTCGCAAGGGAGTTAT	CGGGTAACTGATCCCTCCAACAACGTATTCTC
TCTCTTCTCCTGAAGATCGCAAGGGAGTTAT	CGGGTAACTGATCCCTTCAACAACGTATTCTC
CTCTTCTCCTGAAGATCGCAAGGGAGTTAT	GGGTAACTGATCCCTTCAACAACGTATTCTC
CTCTTCTCCTGAAGATCGCAAGGGAGTTAT	GGGTAACTGATCCCTTCAACAACGTATTCTC
TCTTCTCCTGAAGATCGCAAGGGAGTTAT	GGGTAACTGATCCCTTCAACAACGTATTCTC
CTTCTCCTGAAGATCGCAAGGGAGTTAT	GTAACTGATCCCTTCAACAACGTATTCTC
TTCTCCTGAAGATCGCAAGGGAGTTAT	TAACTGATCCCTTCAACAACGTATTCTC
TCTCTTCTCCTGAAGATCGCAAGGGAGTTA	AACTGATCCCTTCAACAACGTATTCTC
TCTCTTCTCCTGAAGATCGCAAGGGAGTT	AACTGATCCCTTCAACAACGTATTCTC
TCTCTTCTCCTGAAGATCGCAAGGGAGTT	CGGGTAACTGATCCCTTCAACAACGTATTCT
TCTCTTCTCCTGAAGATCGCAAGGGAGT	CGGGTAACTGATCCCTTCAACAACGTATTC
TCTCTTCTCCTGAAGATCGCAAGGGAG	CGGGTAACTGATCCCTTCAACAACGTATT

Protein change

G Q I H S L L L K V A R E L Y K Y L N	S Q G A Q I R E Y V V G G I S Y P L L P
G Q I H S L L L K I A R E L Y K Y L N	S Q G A Q I R E Y V V E G I S Y P L L P

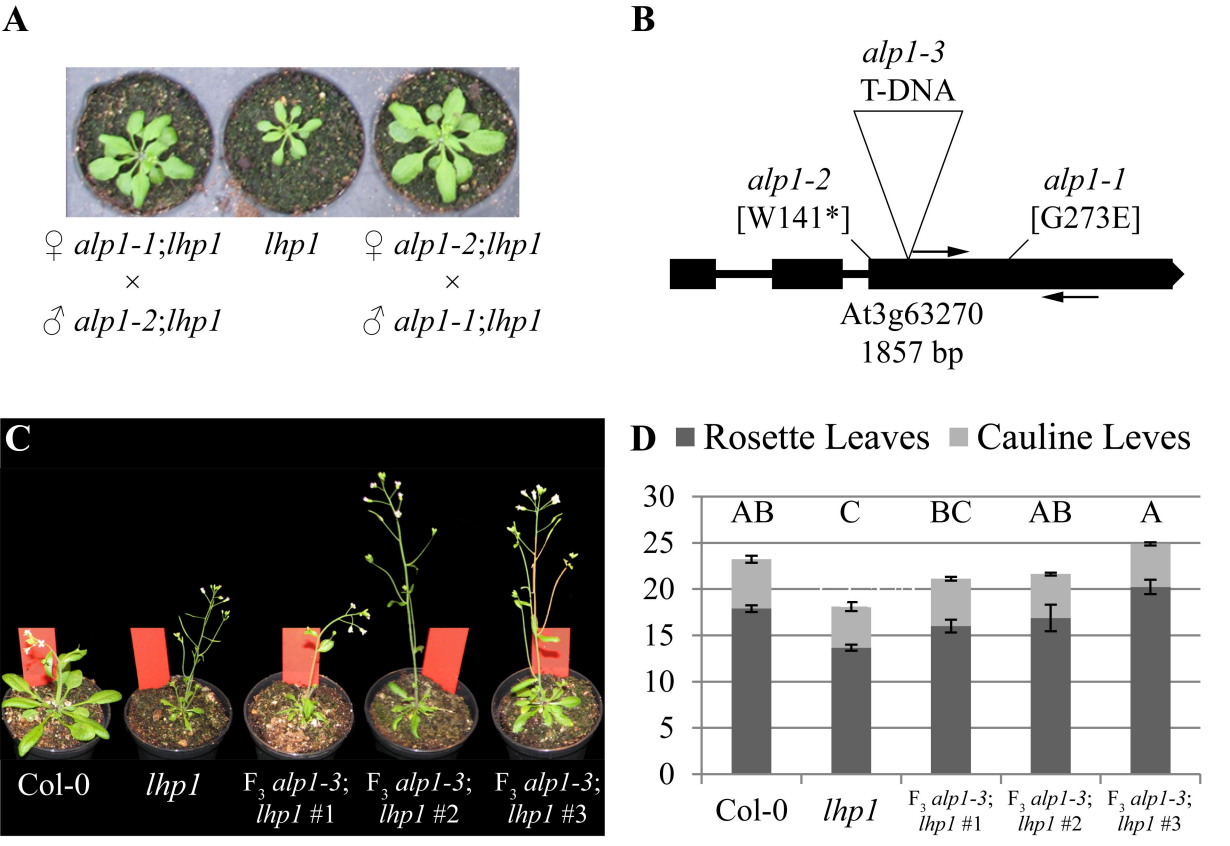
A
♀ alp1-1;lhp1
×
♂ alp1-2;lhp1
lhp1
♀ alp1-2;lhp1
×
♂ alp1-1;lhp1
B
alp1-3
T-DNA
alp1-2
[W141*]
alp1-1
[G273E]
At3g63270
1857 bp
C
Col-0
lhp1
F3 alp1-3; lhp1 #1
F3 alp1-3; lhp1 #2
F3 alp1-3; lhp1 #3
D
Rosette Leaves
Cauline Leves
30
25
20
15
10
5
0
AB
C
BC
AB
A
Col-0
lhp1
F3 alp1-3; lhp1 #1
F3 alp1-3; lhp1 #2
F3 alp1-3; lhp1 #3

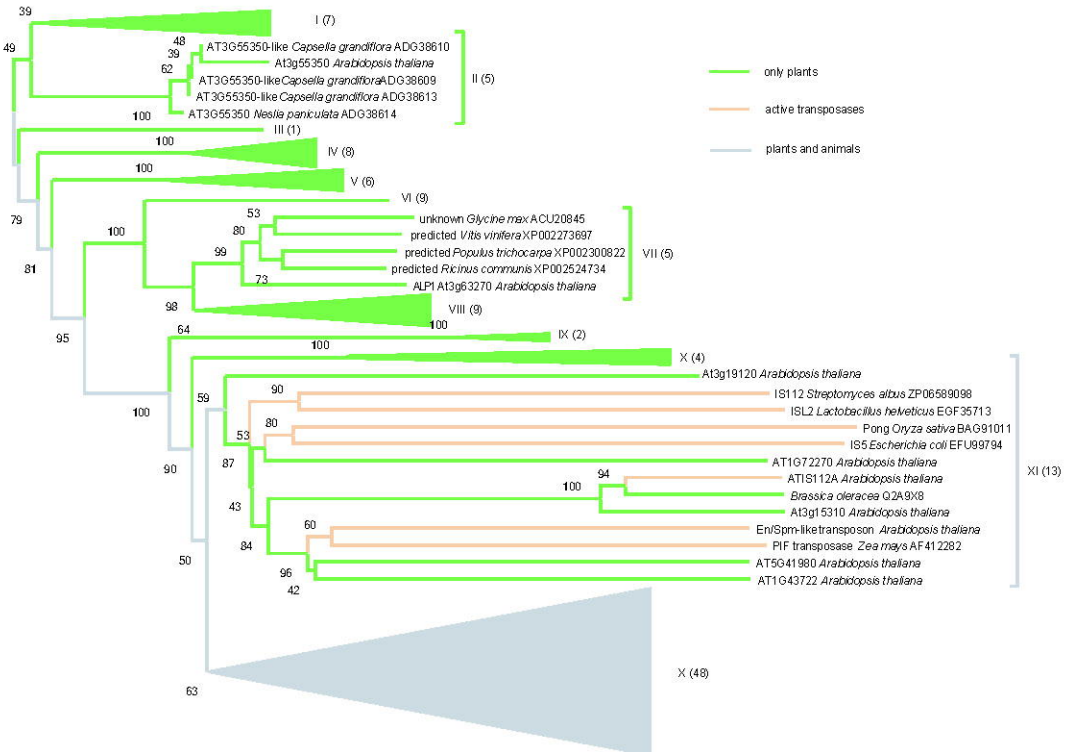
I (7)
AT3G55350-like Capsella grandiflora ADG38610
At3g55350 Arabidopsis thaliana
AT3G55350-like Capsella grandiflora ADG38609
AT3G55350-like Capsella grandiflora ADG38613
AT3G55350 Neslia paniculata ADG38614
II (5)
III (1)
IV (8)
V (6)
VI (9)
unknown Glycine max ACU20845
predicted Vitis vinifera XP002273697
predicted Populus trichocarpa XP002300822
predicted Ricinus communis XP002524734
ALP1 At3g63270 Arabidopsis thaliana
VII (5)
VIII (9)
IX (2)
X (4)
At3g19120 Arabidopsis thaliana
IS112 Streptomyces albus ZP06589098
ISL2 Lactobacillus helveticus EGF35713
Pong Oryza sativa BAG91011
IS5 Escherichia coli EFU99794
AT1G72270 Arabidopsis thaliana
ATIS112A Arabidopsis thaliana
Brassica oleracea Q2A9X8
At3g15310 Arabidopsis thaliana
En/Spm-like transposon Arabidopsis thaliana
PIF transposase Zea mays AF412282
AT5G41980 Arabidopsis thaliana
AT1G43722 Arabidopsis thaliana
XI (13)
X (48)
only plants
active transposases
plants and animals